

Mask-Directed Multiphoton Lithography

Bryan Kaehr and Jason B. Shear*

Department of Chemistry and Biochemistry and the Institute for Cellular and Molecular Biology,
The University of Texas, Austin, Texas 78712

Received December 3, 2006; E-mail: jshear@mail.utexas.edu

We report a strategy for rapidly generating arbitrary microscale patterns of biomaterials that can be used to create complex surface gradients or sequentially assembled into functional three-dimensional microarchitectures. In this approach, mask objects and transparency-based masks are used to direct multiphoton photocrosslinking (MPP) of proteins. Unlike conventional methods for controlling direct-write multiphoton fabrication,¹ this simple graphical-based approach allows new patterns to be created within minutes, enabling rapid iteration and optimization of experimental parameters. We demonstrate use of this strategy to transfer detailed shapes (e.g., the silhouette of a house fly) into biomaterial patterns and to fabricate microchambers capable of trapping and incubating a single motile bacterium.

Multiphoton lithography provides high-resolution microfabrication capabilities in three dimensions, using nonlinear excitation to promote photopolymerization² or protein photocrosslinking^{3,4} within a femtoliter voxel created by tightly focusing a pulsed laser beam. By scanning the fabrication voxel through reagent solution, complex three-dimensional microscale objects^{1,5} have been produced with lateral feature sizes as small as ~ 120 nm using synthetic materials¹ and ~ 250 nm using proteins.⁴

Figure 1A demonstrates our approach for mask-directed multiphoton lithography. Here, light from a femtosecond titanium:sapphire (76 kHz) laser is sent through an unmodified confocal scan box to raster the beam in a rectangular pattern at a focal plane positioned between the scan box and an inverted microscope. This focal plane (mask plane) is conjugate with the front focal plane of the microscope objective. By placing an object (such as *Musca domestica*, Figure 1A) or a pattern printed on transparency film within the mask plane, microstructures representing the object silhouette or mask negative can be fabricated at the objective focal plane. Fabrication objects, created by multiphoton crosslinking of bovine serum albumin (BSA) or other proteins, display feature sizes of $F_{\text{mask}}/M_{\text{obj}}$, where F_{mask} is the feature size in the mask and M_{obj} is the magnification of the objective/lens system. Minimum achievable feature sizes are determined by the spatial confinement of multiphoton absorption and the diffusion distances of reactive intermediates.⁶ From a practical standpoint, masks printed on standard low-resolution transparencies (1200 dpi) can be used with a conventional 100X (1.3 NA) objective to produce features of $\sim 0.5 \mu\text{m}$ (Figure 1A–C)—a scale appropriate for addressing a broad range of applications in cell biology and microtransport.⁷

Using this general approach, multiple masks can be used in concert to fabricate complex patterns containing gradients of crosslinked protein (Figure 1B). Here, a negative transparency photomask was placed in the mask plane to define the microstructure shape and a second fully opaque mask was translated during scanning at a constant velocity to vary the integrated laser exposure across the pattern. This approach allows fabrication of functional gradients (Figure S1) with arbitrary directionality and slope (by changing the direction and speed of the moving mask) with

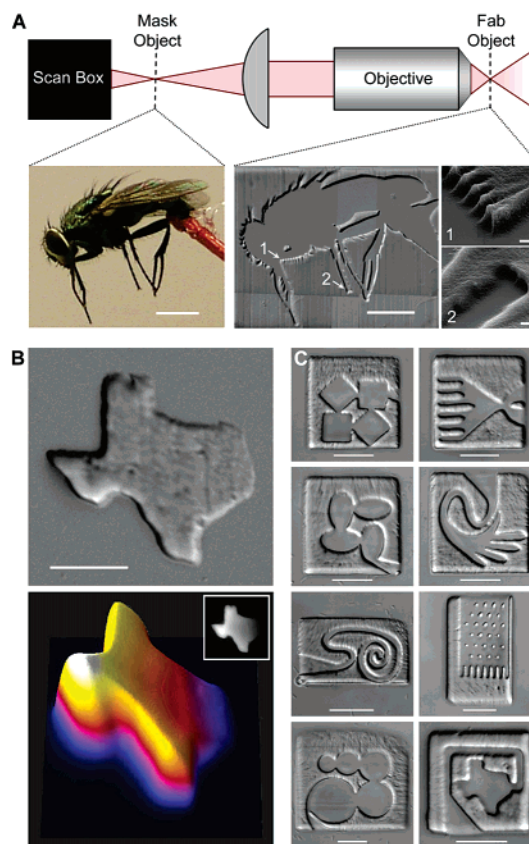


Figure 1. Mask-directed multiphoton lithography. (A) Placement of a mask object (left panel; scale bar, 2 mm) in a plane conjugate to the front focal plane of the microscope objective directs fabrication of the object negative (montage of DIC images, center panel; scale bar, $20 \mu\text{m}$) using multiphoton lithography. Regions demarked 1 and 2 in this image are shown in detail in SEMs (right panels; scale bar, $1 \mu\text{m}$). (B) A linear protein microgradient was fabricated in the shape of a large state using a negative transparency photomask in concert with a mask that was translated during laser scanning. The lower panel is a 3D surface intensity plot of fluorescence (inset) from entrapped photosensitizer. (C) 3D protein microchambers having single entrances and tops sealed by scanning the laser beam without a photomask in place. Scale bars in B and C are $15 \mu\text{m}$.

significantly higher resolution than other techniques that use laser scanning⁸ or broadband light sources.⁹ Our approach is readily adaptable to existing microscope platforms, is potentially inexpensive,¹⁰ and should facilitate studies of cell development and differentiation.

Mask-directed multiphoton lithography enables facile optimization of microfabricated materials for interfacing with cell cultures, such as the capture and incubation of motile cells. By using CAD software and an office printer it was straightforward to rapidly prototype a wide variety of bacterial microchambers, such as those shown in Figure 1C. Such microstructures can be designed to

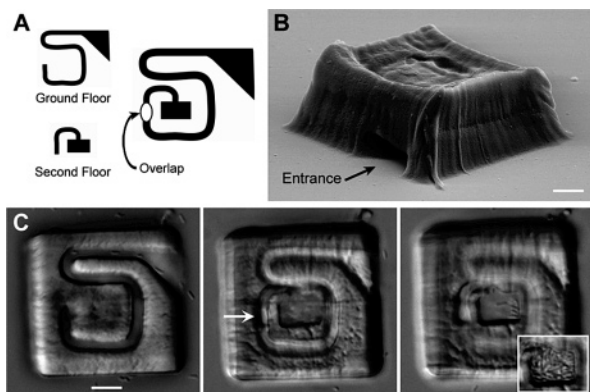


Figure 2. A two-story BSA microstructure fabricated using ground floor and second floor masks sequentially (A). The overlap region shunts bacteria from the ground floor to the second floor loft. (B) SEM of the resultant two-story BSA microstructure. (C) DIC images showing *E. coli* cells (RP9535) entering and transiting the ground floor passage (left panel) to the overlap region (arrow, middle panel) and up to the loft (right panel), which ultimately becomes filled (inset). Scale bars (B, C) are 5 μm .

assemble defined arrays of immobilized cells (e.g., top right) or guide cellular motion (e.g., lower left).

Complex three-dimensional microstructures, such as a two-story microcontainer, also could be fabricated within several minutes using two masks in sequence (Figure 2A). In this device, smooth swimming *E. coli* enter the container through an aperture (Figure 2B–C), and swim through a passageway to the overlap region of the two stories. Here, the bacteria are shunted vertically into the top chamber (see movie S1). Ultimately, cells accumulate to a point that the chamber becomes tightly packed, preventing entry of additional cells (inset). Such bacterial traps may prove to be valuable platforms for studying population-based behaviors¹¹ such as quorum sensing and biofilm formation.

A simple mask was used to create a protein microchamber for single-cell capture and bioincubation, a structure useful for probing cellular properties in controlled environments. Here, a BSA chamber was fabricated with a narrow entrance aperture (Figure 3). Wild-type *E. coli* then was added to the fabrication solution (composed of BSA and the nontoxic photosensitizer, flavin adenine dinucleotide⁴). After a single bacterium entered the chamber, a BSA plug was crosslinked to seal the chamber and trap the cell (a procedure compatible with living cells⁴), allowing cell divisions to be monitored over many hours (movies S2–S4). Although capture and extended incubation of bacterial and yeast cells in addressable microchambers recently has been reported,¹² the procedure relied on a relatively complex soft lithography-based process and required continuous solution flow through the incubation chamber to replenish nutrients and eliminate cell waste. The porosity of photocrosslinked protein matrices allows facile exchange of nutrients and waste into and out of chambers via diffusion,¹³ obviating the need for forced solution flow. Moreover, microchambers can be fabricated rapidly using mask-directed multiphoton lithography, allowing fast optimization of design parameters (e.g., chamber shape, dimensions) important for efficient capture and incubation of motile bacteria and mammalian cells such as neutrophils.

These studies demonstrate the capabilities of mask-directed 3D lithography for rapid prototyping of microarchitectures and chemical gradients. Used in combination with approaches for displaying a nearly unlimited range of biologically active species,^{4,14} it will be straightforward to establish complex gradients of diffusible and

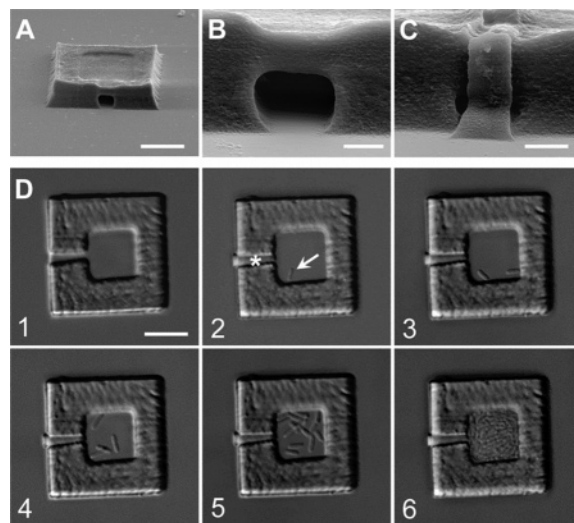


Figure 3. Biocompatible microfabrication allows trapping of a single bacterium. (A, B) SEM images of a BSA microcontainer similar to that shown in parts C and D. (C) SEM of a BSA container after the entrance was plugged with a bacterium inside. (D) Sequence showing a BSA container before (1) and immediately after (2) fabrication of a plug to trap a bacterium (arrow; scale bar, 10 μm). Cell division eventually fills the trap with no loss of bacteria (3–6). Time points are (3) 172 min, (4) 360 min, (5) 590 min, (6) 16 h. Scale bars are A/D, 10 μm ; B/C, 2 μm .

immobilized effectors for interaction with cell cultures. In addition, the possibility for coupling this technology with automated sequencing of masks (e.g., via use of a digital micromirror device in the mask plane¹⁵) will expand the range of microstructure features that can be fabricated.

Acknowledgment. We gratefully acknowledge support from NSF Grant 0317032 and Welch Foundation Grant F-1331. We thank J. Parkinson for *E. coli* strains and helpful advice. J.S. is a Fellow of the Institute for Cellular and Molecular Biology.

Supporting Information Available: Materials and detailed methods; Figure S1; Movies S1–S4. This material is available free of charge via the Internet at <http://pubs.acs.org>.

References

- (1) Kawata, S.; Sun, H.; Tanaka, T.; Takada, K. *Nature* **2001**, *412*, 697–698.
- (2) Maruo, S.; Nakamura, O.; Kawata, S. *Opt. Lett.* **1997**, *22*, 132–134.
- (3) Pitts, J. D.; Campagnola, P. J.; Epling, G. A.; Goodman, S. L. *Macromolecules* **2000**, *33*, 1514–1523.
- (4) Kaehr, B.; Allen, R.; Javier, D. J.; Currie, J.; Shear, J. B. *Proc. Natl. Acad. Sci. U.S.A.* **2004**, *101*, 16104–16108.
- (5) Deubel, M.; von Freymann, G.; Wegener, M.; Pereira, S.; Busch, K.; Soukoulis, C. M. *Nat. Mater.* **2004**, *3*, 444–447.
- (6) Sun, H. B.; Kawata, S. *Adv. Polym. Sci.* **2004**, *170*, 169–273.
- (7) El-Ali, J.; Sorger, P. K.; Jensen, K. F. *Nature* **2006**, *442*, 403–411.
- (8) Hahn, M. S.; Miller, J. S.; West, J. L. *Adv. Mater.* **2005**, *17*, 2939–2942.
- (9) Burdick, J. A.; Khademhosseini, A.; Langer, R. *Langmuir* **2004**, *20*, 5153–5156.
- (10) Kaehr, B.; Ertas, N.; Nielson, R.; Allen, R.; Hill, R. T.; Plenert, M.; Shear, J. B. *Anal. Chem.* **2006**, *78*, 3198–3202.
- (11) Park, S.; Wolanin, P. M.; Yuzbashyan, E. A.; Lin, H.; Darnton, N. C.; Stock, J. B.; Silberzan, P.; Austin, R. *Proc. Natl. Acad. Sci. U.S.A.* **2003**, *100*, 13910–13915.
- (12) Groisman, A.; Lobo, C.; Cho, H.; Campbell, J. K.; Dufour, Y. S.; Stevens, A. M.; Levchenko, A. *Nat. Methods* **2005**, *2*, 685–689.
- (13) Basu, S.; Wolgemuth, C. W.; Campagnola, P. J. *Biomacromolecules* **2004**, *5*, 2347–2357.
- (14) Hill, R. T.; Shear, J. B. *Anal. Chem.* **2006**, *78*, 7022–7026.
- (15) Lu, Y.; Mapili, G.; Suhali, G.; Chen, S.; Roy, K. J. *Biomed. Mater. Res. A* **2006**, *77A*, 396–405.

JA068390Y